Effect of pressure on OH and OD impurities in $LiNbO_3$

1999 J. Phys.: Condens. Matter 11 583

(http://iopscience.iop.org/0953-8984/11/2/021)

J. Phys.: Condens. Matter **11** (1999) 583–591. Printed in the UK PII: S0953-8984(99)96941-2

Effect of pressure on OH and OD impurities in $LiNbO_3$

P G Johannsen†, V Schäferjohann† and S Kapphan‡

† Fachbereich Physik, Universität GH Paderborn, D-33095 Paderborn, Germany
‡ Fachbereich Physik, Universität Osnabrück, D-49069 Osnabrück, Germany

Received 24 August 1998

Abstract. The fundamental vibrational transition frequencies of OH and OD defects, as well as the first OH overtone and the vibrational–librational OH-combination band, are investigated in $LiNbO_3$ under pressure using the diamond-anvil technique. The absorption bands shift to lower wavenumbers and become considerably broader at higher pressures. The experimental results are alternatively discussed within a single oscillator model and a recently developed model for hydrogen bonds in solids.

1. Introduction

Hydrogen impurities in $LiNbO_3$ influence the properties of this technologically important material [1–5]. The OH stretching vibration at about 3500 cm^{-1} is completely polarized perpendicular to the ferroelectric *c*-axis [6], and the overtone spectrum up to the fourth excited state has been determined in congruent and proton exchanged material [7, 8]. From these measurements it was concluded that previously proposed hydrogen bonding of the OH centres [9] appears to be unlikely, because the observed transition energies and line shapes are at variance with the predictions of a traditional double-Morse-potential (DMP) model, usually used for the description of proton states in hydrogen bonds ([10] and references therein). This dismissal of a proton potential according to the DMP model is obviously supported by the fact that from experimental evidence the proton states are localized, in contrast to the delocalized states of the DMP model.

However, it has been recently emphasized [10] that the traditional DMP model is not an optimal description of hydrogen bonds in general. Using a more advanced double-well-potential model it has been demonstrated that hydrogen bonding of the OH centres in $LiNbO_3$ cannot be ruled out. With regards to this pending controversy, one can expect an important contribution from a high-pressure investigation, because, for hydrogen bonds, a strong correlation between the oxygen–oxygen distance and the proton stretching frequency has been noted [11]. These inter-ionic distances can be systematically monitored by high pressure, and the observation of the proton stretching frequency should provide important information as to whether or not OH centres in $LiNbO_3$ follow the systematic behaviour of hydrogen bonds. In the present study, we are reporting on the results of such experiments.

2. Experiment

The present high-pressure experiments were performed in a gasketed diamond-anvil cell (DAC) equipped with type IIa diamonds [12]. The initial hole diameter of the inconel gaskets was

0953-8984/99/020583+09$19.50

300 μm. PCTFE-oil or dry KI-powder was used as pressure transmitting medium and the pressure was determined from the red shift of the ruby fluorescence, using the linear ruby scale [13]. In the Bruker IFS 113v or Bruker HR 120 Fourier-transform spectrometer, tungsten halogen lamps were used together with Si:CaF_2 beamsplitters. The signals were detected by liquid-N_2-cooled InSb detectors.

Transmission spectra using the diamond anvil technique are often obscured by Fabry–Pérot interference fringes, particularly at low pressures [14, 15]. At higher pressures, this effect is less pronounced, because the refractive index of the pressure medium becomes comparable to the refractive index of the diamonds, and, furthermore, the former flat diamond tips become curved. In the present work, the fringes in low-pressure spectra have been reduced by digital filtering [16–18].

In mid-IR experiments, using the DAC technique, absorption in the diamond anvils has to be taken into account. Figure 1(a) shows two typical transmission spectra of type IIa diamonds, whereby the first spectrum was obtained on an empty DAC at ambient conditions. The second spectrum was obtained on the gasketed DAC without a sample, but the pressure medium compressed to 27 GPa. It can be observed that the two- and three-phonon bands are slightly shifted due to the stresses in the anvil tips. Usually, sample spectra are divided by a reference spectrum (e.g. the first spectrum) to remove the background signal. The changes in the diamond absorptions lead thereby to artificial structures, which have to be excluded from the interpretation of the data. Figure 1(b) shows the ratio of the two spectra of part (a), demonstrating that the 100% line is modulated in those parts of the frequency range where the phonon spectra rapidly change (indicated by arrows).

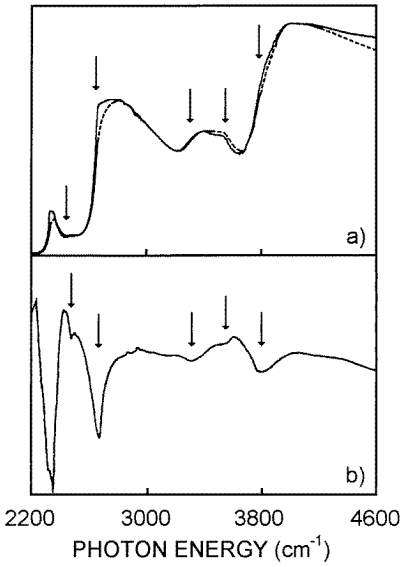

Figure 1. (a) Transmission spectrum of an empty diamond-anvil cell (continuous line), used as reference spectrum in the present experiments, and a spectrum of a gasketed cell with the pressure medium at 27 GPa (broken line). The two- and three-phonon bands shift slightly in the strained anvil tips, giving rise to artificial structures in the 100% line of a sample spectrum. (b) Ratio spectrum (100% line) of the two spectra of part (a). The arrows point to rapid changes of the two- and three-phonon bands, giving rise to these artificial structures.

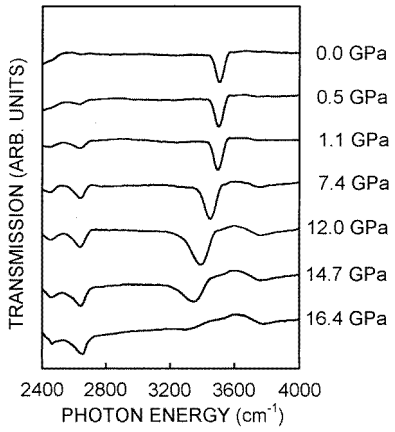

Figure 2. Fundamental OH stretching peak in PE:$LiNbO_3$ under pressure. The peak shifts to lower wave numbers and becomes significantly broader above 10 GPa. In the spectrum at 16.4 GPa, only the artificial diamond features (see figure 1) can be observed.

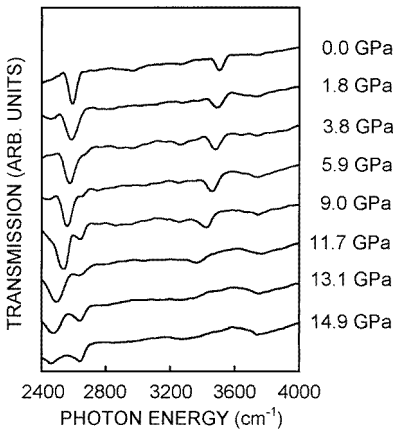

Figure 3. Fundamental OD stretching peak in DE:$LiNbO_3$ under pressure. The peak shifts to lower wave numbers and is increasingly obscured by the diamond artifacts (see figure 1). There is obviously also some amount of OH centres present in this sample.

In the present work, IR spectra have been measured in several runs on proton exchanged $LiNbO_3$ samples (PE), samples of 'as-grown' material with OH in the bulk, and samples of deuteron exchanged material (DE). (PE/DE) $LiNbO_3$ layers have been produced by immersion of thin (thickness $\approx$50 μm) z-cut, congruent $LiNbO_3$ samples [19] in benzoic/fully deuterated benzoic acid melts, buffered with 0.5 mol% lithium benzoate to avoid surface damage, at $T_{PE} = 244\,^{\circ}$C.

The strength of the defect absorption is proportional to the depth of the proton (deuteron) exchanged layer. The optical density was kept well below a value of $\log(I_0/I) < 2$ for the fundamental absorption bands v_{vib}^{01} (figures 2 and 3). For the measurement of the weak overtone absorption v_{vib}^{02} (figure 4), a very high fundamental v_{vib}^{01} absorption, and therefore proton exchanged layers of more than 10 μm depth, had to be employed by treating the samples for up to 200 hours [20]. Care was taken to perform these long treatments in completely sealed quartz crucibles.

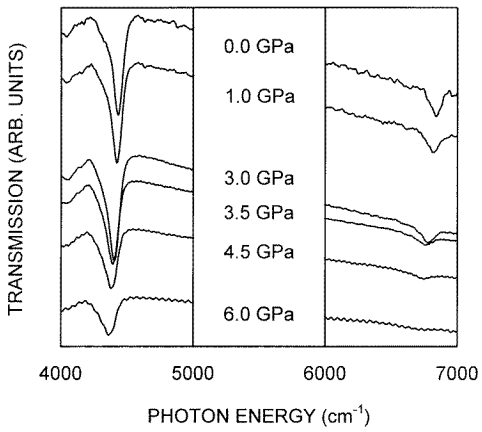

Figure 4. Effect of pressure on the librational–vibrational combination band and the first overtone in PE:$LiNbO_3$.

3. Results and discussion

3.1. Effect of pressure on the transition bands

Figure 2 contains a collection of typical spectra of the fundamental transition in PE:$LiNbO_3$ at different pressures. The ambient-pressure value of the OH stretching peak was 3505 cm^{-1}, which is in good agreement with previous values for proton exchanged materials: 3501 cm^{-1}, 3503 cm^{-1} [7] and 3508 cm^{-1} [8]. Under compression, this peak shifts to lower wavenumbers with increasing pressure and becomes considerably broader above 10 GPa. In the spectrum at 16.4 GPa only the artificial background of the diamonds (figure 1) can be observed.

The peak position at ambient conditions of the $LiNbO_3$ samples with OH in the bulk was somewhat lower: 3483 cm^{-1} (3481 cm^{-1} [7]), but the pressure behaviour was completely analogous to the PE material.

The shift of the fundamental OD peak in the deuteron exchanged material is demonstrated in figure 3. The ambient-pressure value was 2586 cm^{-1} (2589 cm^{-1} [7]). There was also some amount of OH present in this material. The OD peak shifts to lower wavenumbers with increasing pressure and is more and more obscured by the diamond artifact at pressures above 10 GPa.

The shift of the fundamental OH/OD peaks showed a reversible behaviour in pressure cycles up to about 12 GPa. When the samples were taken to higher pressures, the samples started to turn their colour gradually into dark above 20 GPa, and were completely opaque at 30 GPa. Such a behaviour of $LiNbO_3$ has already been reported in [21–23], where a phase transition at 30 GPa, accompanied with a darkening of the samples, had been detected.

When the pressure on those samples, which had been taken to the phase transition, was released, the samples cleared up again, but the behaviour of the OH and OD peaks was different from their behaviour in the upstroke experiments: the peaks reappeared at a pressure of only 5 GPa, showed a somewhat steeper pressure dependence, and remained weak at ambient conditions. Due to these experimental problems we therefore limited our experiments in the present study to the reversible range $p \leqslant 16$ GPa†.

Spectra from the overtone region of the PE material are represented in figure 4. The frequency $\nu_{vib,lib}^{01,01}$ of the vibration–libration combination band [24] (left-hand side) shifts to

† The results are given in table 1

Table 1. Experimental and theoretical frequencies for the fundamental OH and OD stretching modes. The calculated frequencies have been obtained using the model of [10].

PE (exp)		OH in bulk (exp)		DE (exp)				v_{vib}^{01} (cm^{-1})	
p (GPa)	v_{vib}^{01} (cm^{-1})	p (GPa)	v_{vib}^{01} (cm^{-1})	p (GPa)	v_{vib}^{01} (cm^{-1})	p (GPa)	R (pm)	OH (calc)	OD (calc)
0.0	3504	0.0	3483	0.3	2588	0.00	288	3507	2583
0.9	3494	0.9	3480	1.0	2583	1.23	286	3497	2576
1.7	3487	2.0	3468	2.1	2582	2.58	284	3484	2568
2.6	3480	4.3	3449	3.1	2576	4.09	282	3469	2558
3.2	3477	7.1	3418	4.1	2573	5.75	280	3452	2547
4.5	3468	10.1	3371	5.4	2563	7.56	278	3432	2534
5.5	3448	13.7	3300	6.1	2558	9.53	276	3409	2519
7.0	3431			7.0	2550	11.65	274	3381	2502
7.4	3452			8.3	2542	13.94	272	3348	2481
7.4	3434			9.3	2535				
8.1	3419			10.5	2525				
9.2	3413			11.5	2512				
10.9	3389			12.0	2495				
11.7	3379								
11.9	3389								
14.5	3347								

Table 2. Experimental frequencies of the vibrational–librational combination band and of the first overtone in PE:$LiNbO_3$. Theoretical values according to the model of [10] are also given.

PE (exp)		PE (exp)				v_{vib}^{02} (cm^{-1})	
p (GPa)	$v_{vib,lib}^{01,01}$ (cm^{-1})	p (GPa)	v_{vib}^{02} (cm^{-1})	p (GPa)	R (pm)	OH (calc)	OD (calc)
0.0	4435	0.0	6840	0.00	288	6847	5083
1.0	4425	1.0	6820	1.23	286	6820	5066
3.0	4410	3.0	6780	2.58	284	6789	5053
3.5	4400	3.5	6765	4.09	282	6752	5025
4.5	4390	4.5	6745	5.75	280	6708	5000
6.0	4375	6.0	6700	7.56	278	6656	4970
				9.53	276	6591	4934
				11.65	274	6508	4892

lower wavenumbers and the lineshape of this band becomes considerably broader at about 6 GPa. There are different effects which may contribute to the frequency change [24]

$$v_{vib,lib}^{01,01}(p) = v_{vib}^{01}(p) + v_{lib}^{01}(p)\left(\frac{\langle\Psi_1|1/r^2|\Psi_1\rangle}{\langle\Psi_0|1/r^2|\Psi_0\rangle}\right)^{1/2}. \quad (1)$$

$v_{vib}^{01}(p)$ is known from the above experiments and will be discussed in more detail in sections 3.2 and 3.3. Under the assumption that the ratio of the matrix elements in equation (1) is constant with pressure, it is the variation of the librational frequency $v_{lib}^{01}(p)$, which contributes to $v_{vib,lib}^{01,01}(p)$. On the one-hand side, $v_{lib}^{01}(p)$ is a function of the force constant for the librational motion, and on the other hand, it may also depend on the change of the moment of inertia due to a possible change of the intra-molecular separation r_{OH}. These two contributions are not known

for the system under consideration, but some conclusions may be drawn from the observed frequency differences $v_{vib,lib}^{01,01}(p) - v_{vib}^{01}(p)$, which have a constant value of 927(3) cm^{-1} within experimental accuracy†.

Within the local oscillator model (see section 3.2), the inter-nuclear distance r_{OH} is not important for the description of the stretching frequencies. Therefore, according to this model, one can conclude that the possible changes in the force constant of the librational motion and possible changes of the inter-nuclear distance result in a constant contribution to the frequency of the combination band.

In hydrogen bonds (see section 3.3), on the other hand, the inter-nuclear distance r_{OH} depends on the space R between the two neighbouring oxygen atoms [10, 11], increasing with decreasing R or increasing pressure. Therefore, according to this model, it can be concluded that the force constant of the librational motion increases with increasing pressure.

3.2. Local oscillator model

Hydrogen bonds have been described in the literature nearly exclusively by the DMP model. The proton states in such symmetric potentials are delocalized with equal probability in both wells, but in the OH:$LiNbO_3$ system localized proton states have to be concluded from experimental evidence. Furthermore, in proton-exchanged material it was possible to determine the overtone spectrum up to the third overtone. The detected frequencies and line shapes are at variance with the predictions of the DMP model. Therefore, a local-oscillator model was proposed in [8].

In this local-oscillator model, the proton potential is described by a Morse function $V(r) = D_e(1 - e^{-a(r-r_e)})^2$, and the transition frequencies from the ground state to the nth excited state are given by [25]

$$\bar{v}_{0n} = n\omega_e - (n^2 + n)\omega_e x_e \tag{2}$$

with

$$\omega_e = a\sqrt{2D_e/\mu_m} \qquad \omega_e x_e = a^2 h/(4\pi\mu_m). \tag{3}$$

μ_m is the reduced mass, $r_e = 96$ pm the OH nuclear equilibrium separation, D_e the potential depth and h Planck's constant. In [8] the values $\omega_e = 3684$ cm^{-1} and $\omega_e x_e = 88.5$ cm^{-1} were determined, which correspond to the potential parameter values $D_e = 4.75$ eV and $a = 22.23$ nm^{-1}. Within this model, the fundamental transition frequency, as well as the next three overtones of OH and OD centres in $LiNbO_3$ can be described within experimental accuracy [8].

This local oscillator model uses the two model parameters D_e and a. The description of the observed pressure dependence of the stretching frequencies can therefore be evaluated in terms of pressure dependent parameters $D_e = D_e(p)$ and $a = a(p)$. By means of both the information on the fundamental stretching frequency and the first overtone, it is thereby possible to derive the pressure dependencies of the two parameters independently. It turns out that the parameter a is constant within experimental accuracy and the frequency shifts can be described by a linear pressure dependence

$$D_e = D_{e0}(1 - bp). \tag{4}$$

Figure 5 shows the observed experimental values of the stretching frequencies and different theoretical approaches. It can be observed that a linear decrease of the parameter D_e, with $D_{e0} = 4.75$ eV and $b = 0.0055(2)$ GPa^{-1}, which corresponds to a mode-Grüneisen

† Results are given in table 2

parameter of $\gamma = (K/v)\,\mathrm{d}v/\mathrm{d}p = -0.41(2)$ (with the bulk modulus $K = 134$ GPa of [21]), represents the experimentally observed variation of the stretching frequencies within experimental accuracy.

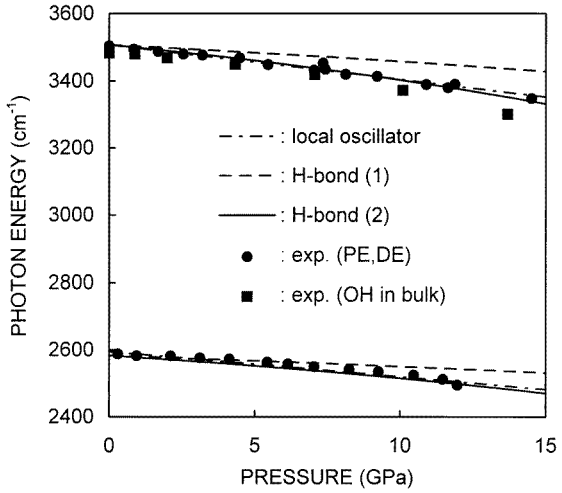

Figure 5. Effect of pressure on the fundamental OH and OD stretching frequencies in PE:$LiNbO_3$ and DE:$LiNbO_3$ (circles) and bulk OH:$LiNbO_3$ (squares), whereby the point sizes represent approximately the experimental uncertainties. The chain lines indicate fits of the local oscillator model to the experimental data according to the equations (2)–(4). The broken lines represent the frequency shifts, calculated with the model of [10], under the assumption $\frac{R}{R_0}(p) = \frac{a}{a_0}(p)$. The continuous lines have been obtained on the assumption that the O–O distance in hydrogen bonds decreases more strongly under compression than the other O–O distances (see the text).

3.3. Hydrogen bonding

It has been demonstrated in [10] that the DMP model, although frequently in use, is not an optimal representation of the proton potential in hydrogen bonds in general. On the one hand, delocalized proton states in solids have to be regarded as rare and exceptional cases, and, on the other hand, the double-Morse function with a certain set of parameters is only a quantitative representation for a limited range of the bond length. Using a more advanced non-symmetric potential with localized proton states, it has been shown in [10] that the overtone spectrum of [8], which cannot be explained with the traditional DMP, is not in contradiction to the assumption of a generalized double-well potential. This model [10] predicts a negative mode-Grüneisen parameter, and it is therefore natural to apply this model to the present results.

The model of [10] describes the frequencies and line intensities and widths depending on the oxygen–oxygen distance R. In special cases (e.g. H_2O ice), this bond length can be related to pressure, using the respective equation of state. However, in the present case, there is only limited information about the position of the protons and its possible oxygen neighbours. From the polarization dependence of the absorption it was concluded that the stretching motion takes place perpendicular to the c-axes [6]. In this plane, several oxygen–oxygen distances are observed at ambient conditions [6], and, if the OH^--ion occupies a regular oxygen lattice site, several distances to neighbouring oxygen ions are therefore possible. However, the frequency of about 3500 cm^{-1} points to an O–O bond length of about $R \approx 290$ pm [10, 11].

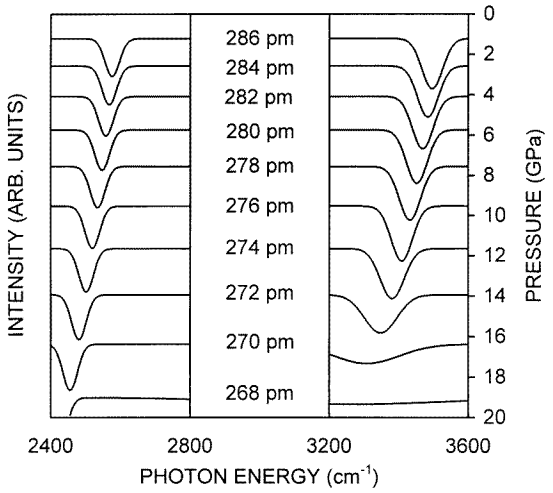

Figure 6. Calculated variation of the fundamental OD- and OH-absorption line according to the model of [10]. The pressure scale corresponds to the continuous lines in figure 5, and the corresponding bond lengths R are also given.

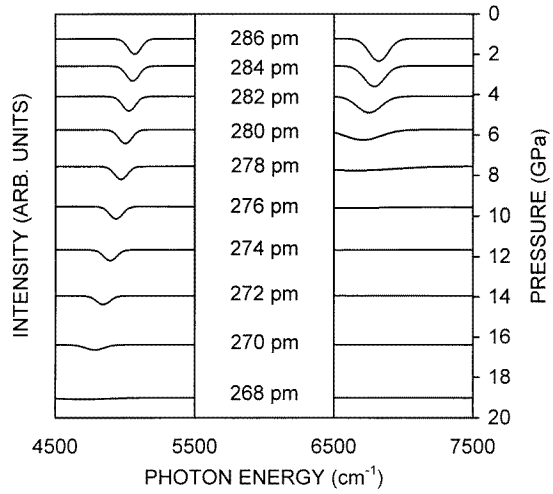

Figure 7. Calculated line shifts and line broadenings of the first OD and OH overtone according to the model of [10].

The equation of state and the variation of the c/a-ratio with pressure have been determined in [21]. From these data, the variation of the a-axes with pressure can be extracted, and, in a first approach, it may be assumed that the change of the bond length R is proportional to the variation of the a-axes $(R/R_0)(p) = (a/a_0)(p)$. One may then calculate the variation of the stretching frequency according to the model of [10]. Figure 5 shows also the prediction of this model with the above mentioned assumption. It can be noted that the experimental frequencies decrease more rapidly than predicted by the model. It must therefore be concluded that the bond length is more strongly reduced than the other oxygen–oxygen distances in this plane. This is not completely unexpected, because the protons should reduce the repulsive forces between two neighbouring oxygen ions.

Therefore, in a second approach, one may take the observed frequencies for the determination of the bond-length variation. This can be obtained by scaling the bond-length variation by a constant factor $(\Delta R/R_0)(p) = c(\Delta a/a_0)(p)$, with $c = 1.9$ in the present case. It can also be observed in figure 5 that the observed and calculated frequencies can thereby be brought into satisfactory agreement (see tables 1 and 2). The mode-Grüneisen parameter $\gamma = 0.32(2)$ is somewhat lower than in the local oscillator model.

The model of [10] allows also for the calculation of line intensities and widths. The results of these calculations are represented in figure 6. It can be noted that the model predicts line broadening of the proton peak at about 15 GPa, which is obviously in excellent agreement with the experimental findings (figure 2).

Within the model of [10], line broadening is related to incoherent tunnelling of the protons in states which are energetically near the barrier top of a double minimum potential. Therefore, the measurement of the first overtone is of particular importance, because the second excited state must be affected by this effect at considerably lower pressures, than the first excited state. Figure 7 shows the calculated variation of the first OH and OD overtones. It can be noticed that considerable line broadening of the OH overtone is predicted already at about 6 GPa, which is obviously in excellent agreement with the experimental findings (figure 4).

In conclusion, the observed line shifts can be described, on the one hand, by a linear pressure dependence of the parameter D_e in the local oscillator model. On the other hand, the assumption of hydrogen bonding is able to describe in addition the observed line broadenings, and the results of the present study can therefore be regarded as an argument in favour of hydrogen bonding.

References

[1] Vormann H, Weber G, Kapphan S and Krätzig E 1981 *Solid State Commun.* **40** 543
[2] Jackel J L, Rice C E and Veselka J J 1982 *Appl. Phys. Lett.* **41** 607
[3] Schmidt N, Betzler K, Grabs M, Kapphan S and Klose F 1989 *J. Appl. Phys.* **65** 1253
[4] Moretti P, Thevenard P, Wirl K, Hertel P, Hesse H, Krätzig E and Godefroy G 1992 *Ferroelectrics* **128** 13
[5] Klauer S, Wöhlecke M and Kapphan S 1992 *Phys. Rev.* B **45** 2786
[6] Herrington J R, Dischler B, Räuber A and Schneider J 1973 *Solid State Commun.* **12** 351
[7] Förster A, Kapphan S and Wöhlecke M 1987 *Phys. Status Solidi* b **143** 755
[8] Gröne A and Kapphan S 1995 *J. Phys.: Condens. Matter* **7** 6393
[9] Loni A, De La Rue R M and Winfield J M 1987 *J. Appl. Phys.* **61** 64
[10] Johannsen P G 1998 *J. Phys.: Condens. Matter* **10** 2241
[11] Novak A 1974 *Struct. Bonding* **18** 177 and references therein
[12] Johannsen P G 1989 *Simple Molecular Systems at Very High Density* ed A Polian *et al* (New York: Plenum) p 277
[13] Piermarini G J, Block S, Barnett J D and Forman R A 1975 *J. Appl. Phys.* **46** 2774
[14] Johannsen P G 1993 *Meas. Sci. Technol.* **4** 237
[15] Johannsen P G, Reiß G, Bohle U, Magiera J, Müller R, Spiekermann H and Holzapfel W B 1997 *Phys. Rev.* B **55** 6865
[16] Gaskill J D 1978 *Linear Systems, Fourier Transforms and Optics* (New York: Wiley)
[17] Bromba M U A and Ziegler H 1984 *Anal. Chem.* **56** 2052
[18] Biermann G and Ziegler H 1986 *Anal. Chem.* **58** 536
[19] Crystal Technology
[20] Kapphan S and Breitkopf A 1992 *Phys. Status Solidi* a **133** 159
[21] da Jornada J A H, Block S, Mauer F A and Piermarini G J 1985 *J. Appl. Phys.* **57** 842
[22] Goto T and Syono Y 1985 *J. Appl. Phys.* **58** 2548
[23] Jayaraman A and Ballman A A 1986 *J. Appl. Phys.* **60** 1208
[24] Gröne A and Kapphan S 1995 *J. Phys.: Condens. Matter* **7** 3051
[25] Morse P M 1929 *Phys. Rev.* **34** 57